Protonation-State-Dependent Luminescence and Excited-State Electron-Transfer Reactions of 2- and 4-Pyridine (-ium)-Substituted Metallo-1,2-enedithiolates

Sharada P. Kaiwar, Anthony Vodacek, Neil V. Blough,* and Robert S. Pilato*

Contribution from the The Department of Chemistry and Biochemistry, The University of Maryland, College Park, Maryland 20742

Received March 14, 1997[⊗]

Abstract: Luminescence and excited-state electron-transfer reactions of (dppe)Pt{S_2C_2(2-pyridine)(H)} and (dppe)-Pt{S_2C_2(4-pyridine)(H)} (dppe = diphenyldiphosphinoethane) are enabled by protonation of the appended pyridine, thus serving as a novel means of electronic switching. The neutral complexes have low-lying d-to-d transitions that lead to rapid decay of excited states by nonradiative processes. However, upon protonation, a 1,2-enedithiolate-to-heterocycle π^* intraligand charge-transfer transition (ILCT) becomes lower in energy than the d-to-d transition, thus giving rise to emissive ^{1}ILCT* and ^{3}ILCT* excited states for [(dppe)Pt{S_2C_2(2-pyridinium)(H)}][BF_4] and [(dppe)-Pt{S_2C_2(4-pyridinium)(H)}][BF_4]. The assignment of these excited states was based on their energies and lifetimes (τ) which range from τ = 3 to 4 ns for the singlet and from τ = 2000 to 7500 ns for the triplet, respectively. Emission quantum yields (ϕ) increase with solvent polarity and range from ϕ = 0.0006 to 0.003 for the singlet and from ϕ = 0.001 to 0.03 for the triplet. The electron acceptors *p*-dinitrobenzene and tetracyanoquinodimethane quench the ^{3}ILCT* with k_q values of 4×10^9 and 9×10^9 M^{-1} s^{-1}, respectively. The k_q values are nearly identical for the 2- and 4-pyridinium complexes, reflecting the similarity in the thermodynamic driving forces for electron transfer from these complexes. The ability to employ a simple and reversible ground-state reaction (ligand protonation) to control access to reactive excited states should prove useful in numerous applications.

Introduction

Transition metal complexes that are luminescent in solution at room temperature have been used in a variety of chemical and biochemical applications.[1−13] Many of these applications require that these complexes act as switching devices whose ability to luminescence and undergo excited-state electron transfer depends on the oxidation state of the metal.[9−12]

Here we demonstrate that the luminescence and excited-state electron-transfer reactions of (dppe)Pt{S_2C_2(heterocycle)(H)} (where dppe = diphenyldiphosphinoethane, heterocycle = 2- and 4-pyridine) depend on the protonation state of the pyridine. The "switching" in these compounds results from a change in the ordering of the electronic transitions in the pyridine- and pyridinium-substituted complexes. In the neutral complexes, a low-lying d-to-d transition leads to the rapid, nonradiative decay of the excited states. Upon protonation, a 1,2-enedithiolate-to-heterocycle π^* intraligand charge transfer (ILCT) becomes the low-lying transition. As has been demonstrated in a previous study,[14b] (dppe)Pt{S_2C_2(heterocycle)(H)} complexes with lowest-lying ILCT transitions exhibit room-temperature luminescence from ^{1}ILCT* and ^{3}ILCT* excited states. Consistent with our previous findings, the long-lived ^{3}ILCT* of the pyridinium-substituted complexes undergoes facile excited-state electron transfer with appropriate electron acceptors.

Experimental Section

Materials. dppeM{S_2C_2(heterocycle)(H)}, 2-pyridine, 3-pyridine, and 4-pyridine were prepared according to the literature procedures.[14,16,17] Tetracyanoquinodimethane (TCNQ) and p-dinitrobenzene (DNB) were purchased from Acros Chemical. HBF_4−etherate (54%) was purchased from Fluka Chemika and used as received. All reactions were performed under an atmosphere of nitrogen using standard Schlenk line techniques. Workups were performed in air unless stated otherwise. Dichloromethane, dichloroethane, acetonitrile, and toluene were dried over calcium hydride and distilled under nitrogen. Dioxane was dried over sodium/benzophenone and distilled under nitrogen. DMF and DMSO were dried over calcium hydride and vacuum distilled. Triethylamine was dried over potassium hydroxide and vacuum distilled.

[⊗] Abstract published in *Advance ACS Abstracts,* September 15, 1997.

(1) (a) Nocera, D. G.; Winkler, J. R.; Yocom, K. M.; Bordignon, E.; Gray, H. B. *J. Am. Chem. Soc.* **1984**, *106*, 5145−50. (b) Chang, I.-J.; Gray, H. B.; Winkler, J. R. *J. Am. Chem. Soc.* **1991**, *113*, 7056−7. (c) Meier, M.; Eldik, R. V.; Chang, I.-J.; Mines, G. A.; Wuttje, D. S.; Winkler, J. R.; Gray, H. B. *J. Am. Chem. Soc.* **1994**, *116*, 1577−8. (d) Beratan, D. N.; Onuchic, J. N.; Betts, J. N.; Bowler, B. E.; Gray, H. B. *J. Am. Chem. Soc.* **1990**, *112*, 7915−21. (e) Lieber, C. M.; Karas, J. L.; Gray, H. B. *J. Am. Chem. Soc.* **1987**, *109*, 3778−9. (f) (17) Sabatani, E.; Nikol, H. D.; Gray, H. B.; Anson, F. C. *J. Am. Chem. Soc.* **1996**, *118*, 1158−63.

(2) Noffsinger, J. B.; Danielson, N. D. *Anal. Chem.* **1987**, *59*, 865−8.

(3) Arena, G.; Scolaro, L. M.; Pasternack, R. F.; Romeo, R. *Inorg. Chem.* **1995**, *34*, 2994−3002.

(4) Kavarnos, G. J.; Turro, N. J. *Chem. Rev.* **1986**, *86*, 401−9.

(5) (a) Pyle, A. M.; Rehmann, J. P.; Meshoyrer, R.; Kumar, C. V.; Turro, N. J.; Barton, J. K. *J. Am. Chem. Soc.* **1989**, *111*, 3051−8. (b) Friedman, A. E.; Chambron, J.-C.; Sauvage, J.-P.; Turro, N. J.; Barton, J. K. *J. Am. Chem. Soc.* **1990**, *112*, 4960−2.

(6) Ledney, M. I.; Dutta, P. K. *J. Am. Chem. Soc.* **1995**, *117*, 7687−95.

(7) Sykora, J.; Sima, J. *Coord. Chem. Rev.* **1990**, *107*, 1−192.

(8) Juris, A.; Balzani, V.; Barigelletti, F.; Campagna, S.; Belser, P.; Von Zelewsky, A. *Coord. Chem. Rev* **1988**, *84*, 85−277.

(9) (a) Liang, P.; Dong, L.; Martin, M. T. *J. Am. Chem. Soc.* **1996**, *118*, 9198−9. (b) Liang, P.; Sanchez, R. I.; Martin, M. T. *Anal. Chem.* **1996**, *68*, 2426−31.

(10) (a) Blackburn, G. G.; Shah, H. P.; Kenten, J. H.; Leland, J.; Kamin, R. K.; Wilkins, E.; Wu, T.-T.; Massey, R. J. *J. Clin. Chem* **1991**, *37*, 1534−9. (b) Leland, J. K.; Powell, J. M. *J. Electrochem. Soc.* **1990**, *1990*, 3127−31.

(11) Knight, W. W.; Greenway, G. M. *Analyst* **1994**, *119*, 879−90.

(12) Ege, D.; Becker, W. G.; Bard, A. J. *Anal. Chem.* **1984**, *56*, 2413−7

(13) a) de Silva, A. P.; Gunaratne, H. Q. N.; Rice, T. E. *Angew. Chem., Int. Ed. Engl.* **1996**, *35*, 2116−8. (b) Sammes, P. G.; Yahioglu, G.; Yearwood, G. D. *J. Chem. Soc., Chem. Commun* **1992**, 1282−3.

(14) (a) Hsu, J. K.; Bonangelino, C. J.; Kaiwar, S. P.; Boggs, C. M.; Fettinger, J. C.; Pilato, R. S. *Inorg. Chem.* **1996**, *35*, 4743−51. (b) Kaiwar, S. P.; Vodacek, A.; Blough, N. V.; Pilato, R. S. *J. Am. Chem. Soc.* **1997**, *119*, 3311−6. (c) Kaiwar, S. P.; Hsu, J. K.; Liable-Sands, L. M.; Rheingold, A. L.; Pilato, R. S. *Inorg. Chem.*, in press.

S0002-7863(97)00834-2 CCC: $14.00

Physical Measurements. UV−visible spectra were recorded on either a Perkin Elmer Lambda 2S or a Hewlet Packard 8452A spectrometer. All electrochemical experiments were conducted on a BAS-50 in either cyclic voltametry (CV) or Osteryoung square wave voltametry (OSWV) modes with 0.1 M $[Bu_4N][PF_6]$ as the supporting electrolyte. In all electrochemical experiments, the electrodes were a carbon working, platinum auxiliary, and Ag/AgCl reference. All electrochemical experiments were conducted in DMSO, where the ferrocene/ferrocenium couple was found at 545 mV.

Luminescence Measurements. Room-temperature excitation and emission spectra were acquired with a SLM AB2 fluorescence spectrometer. Emission spectra were corrected for instrumental response using factors supplied by the manufacturer. Oxygen-free luminescence measurements were made on 10^{-5} M solutions of all complexes that were deoxygenated by three freeze−pump−thaw N_2-backfill cycles in a fluorescence cell equipped with a reservoir and a Teflon valve. Quantum yields, ϕ, were calculated relative to Zn(tpp)-{$\phi_{std} = 0.04$} (tpp = tetraphenylporphyrinato)[15] in air and under Ar.

Luminescent lifetimes of **10** and **14** were acquired with an ISS K2 digital frequency domain spectrofluorometer. The excitation source was a 300 W xenon lamp, and the bandpass of the excitation monochromator was 16 nm. Sample and reference solutions were contained in 1 cm quartz cells at room temperature. A scattering solution of glycogen in Milli-Q water was used as the reference. For some low-intensity samples, a neutral density filter was used to reduce the intensity of the reference scatter. Single-channel detection at 90° was employed, with longpass filters used to block the excitation line and Raman scatter from the sample. Lifetimes were determined from the frequency dependence of the signal phase shifts and demodulation, relative to the reference, using the ISS least-squares analysis software. The minimization procedure assumed discrete lifetimes. The procedure provided lifetimes, fractional photon contributions, and χ^2 for the least-squares fit.

Triplet Quenching Experiments. Second-order rate constants (k_q) for the quenching of the ^{3}ILCT* emission of **10** and **14** (10^{-5} M in DMSO) by *p*-dinitrobenzene (DNB) and tetracyanoquinodimethane (TCNQ) were obtained from plots of I_o/I vs [Q] using the Stern−Volmer equation,

$$I_o/I = 1 + k_q\tau[Q] \qquad (1)$$

where I_o was the emission intensity of the ^{3}ILCT* in the absence of a quenching agent, I was the emission intensity of the ^{3}ILCT* at some quencher concentration [Q], and τ was the lifetime of **10** or **14**, respectively, in the absence of a quenching agent. The uncertainties in k_q were propagated from the standard deviation of the slope and the estimated uncertainties in τ and are reported at the 95% confidence limit.

The second-order rate constants for dioxygen quenching ($k_q(O_2)$) of the ^{3}ILCT* were estimated from the emission percentages (in air and Ar) and the solubilities of dioxygen at 152 Torr in dimethylsulfoxide (DMSO) and acetone.[21]

Results and Discussion

The metallo-1,2-enedithiolate complexes (dppe)M{S_2C_2-(heterocycle)(H)} (where dppe = diphenyldiphosphinoethane, heterocycle = 2-, 3-, and 4-pyridine, and M = Ni, Pd, and Pt, Scheme 1) were prepared by a previously described method.[14a,c]

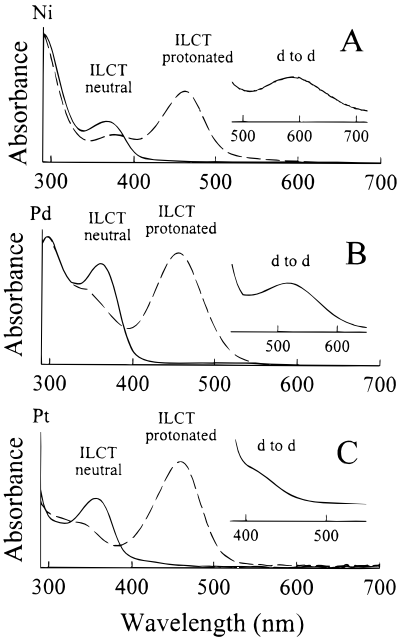

Figure 1. UV−visible absorption spectra: (A) **1** (solid) and **8** (dashed); **(B) 2** (solid) and **9** (dashed); (C) **3** (solid) and **10** (dashed). Insets A−C are expansions of the region of the UV−visible spectrum assigned to the d-to-d transitions of **1**−**3**, respectively.

Scheme 1

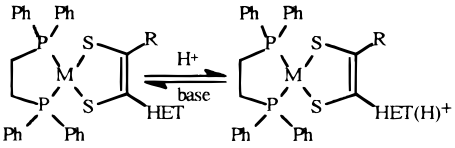

HET	M		
2-pyridine	Ni, Pd, Pt	**1, 2, 3**	**8, 9, 10**
3-pyridine	Ni, Pd, Pt	**4, 5, 6**	**11, 12, 13**
4-pyridine	Pt	**7**	**14**

The protonated complexes **8**−**14** were generated quantitatively as the tetrafluoroborate salts by the addition of 54% HBF_4·etherate to solutions of **1**−**7**, respectively.

Absorption and Emission Properties of 1−14. Consistent with the findings for other heterocyclic substituted metallo-1,2-enedithiolates, including $Cp_2Mo\{S_2C_2$(heterocycle)(H)} (where heterocycle = 2-quinoxaline, 2-, 3-, and 4-pyridine(-ium))[14a] and (dppe)Pt[S_2C_2{2-quinoxaline(ium)}{R}][14b,c] (where R = H, Me, **1**−**7** exhibit an absorption band that can be assigned to a 1,2-dithiolate-to-heterocycle π^* intraligand charge-transfer transition (ILCT) (Table 1). The energy of this band is sensitive to solvent polarity, decreasing by 1000 cm^{-1} for the neutral complexes and increasing by 1000 cm^{-1} for the protonated complexes over the solvent polarity range from CCl_4 to DMSO. While the solvent sensitivity supports assignment to either an ILCT, MLCT (metal-to-ligand charge transfer), or LMCT (ligand-to-metal charge transfer) transition, the energies of this band are nearly identical for the corresponding Ni, Pd, and Pt complexes, thus ruling out a MLCT or LMCT assignment (Table

(15) (a) Quimby, D. J.; Longo, F. R. *J. Am. Chem. Soc.* **1975**, *97*, 5111−7. (b) Harriman, A. J. *J. Chem. Soc., Faraday Trans. I* **1980**, *76*, 1978−85.

(16) (a) Schmidt, M.; Hoffmann, G. G. *Z. Naturforsch B* **1978**, *33*, 1332−37. (b) Schmidt, M.; Hoffmann, G. G.; Holler, R. *Inorg. Chim. Acta* **1979**, *32*, L19−L20.

(17) Menasse, R. v.; Klein, G.; Erlenmeyer, H. *Helv. Chim. Acta* **1955**, *38*, 1289−91.

(18) (a) Shupack, S. I.; Billig, E. C.; Williams, R.; Gray, H. B. *J. Am. Chem. Soc.* **1964**, *86*, 4594−602. (b) Gray, H. B.; Ballhausen, C. J. *J. Am. Chem. Soc.* **1963**, *85*, 260−4. (c) Werden, B. G.; Billig, E.; Gray, H. B. *Inorg. Chem.* **1966**, *5*, 78. (d) Fackler, J. P.; Coucouvanis, D. J. *J. Am. Chem. Soc.* **1966**, *88*, 3913. (e) Bowmaker, G. A.; Boyd, P. D. W.; Campbell, G. K. *Inorg. Chem.* **1983**, *22*, 1208−13.

(19) (a) The energy shifts with solvent polarity correlated poorly with both E_{MLCT^*} and π^*, further supporting the ILCT assignment. (b) Manuta, D. M.; Lees, A. J. *Inorg. Chem.* **1983**, *22*, 3825−8.

(20) While the 3-pyridinium-substituted complex, **13**, has a weak visible band at nearly the same energy as the ILCT band of **10** and **14**, the solvent sensitivity of this band (decreasing with solvent polarity) supports an alternative assignment. The band at 374 nm in the spectrum of **13** has an extinction coefficient and solvent sensitivity similar to those of the bands of **10** and **14** and has been assigned to the ILCT transition. The small shift in the ILCT energy upon the protonation of **4**−**6** (~2100 cm^{-1}) relative to those of **1**−**3** and **7** (6100−6700 cm^{-1}) is attributed to a lack of resonance stabilization of 3-pyridinium by the metallo-1, 2-enedithiolate.[14a,b]

(21) Murov, S. L.; Carmichael, I.; Hug, G. L *Handbook of Photochemistry* 2ed.; Marcel Dekker, Inc.: New York, 1993; pp 289−93.

(22) Bard, A. J.; Faulkner, L. R. *Electrochemical Methods: Fundamentals and Applications*; John Wiley and Sons: New York, 1980.

Table 1. UV−Visible Transitions of Complexes **1**−14 Recorded in CH_2Cl_2

			λ_{max} (ϵ)[a]	
complex	M	R, R′	neutral	protonated
1, **8**	Ni	2-py, H	*367* (4540), 584 (90)	376 (2680), *462* (6960)
2, **9**	Pd	2-py, H	*360* (4000), 519 (90)	343 (sh, 3200), *456* (5690)
3, **10**	Pt	2-py, H	*358* (4300), 415 (sh, 380)	336 (sh, 2800), *458* (6620)
4, **11**	Ni	3-py, H	312 (6030), *358* (4850), 586 (90)	312 (6070), *378* (5820), 444 (sh, 2050)
5, **12**	Pd	3-py, H	298 (6330), *352* (4400), 520 (80)	302 (6630), *382* (4580), 446 (sh, 1610)
6, **13**	Pt	3-py, H	282 (7480), *346* (6040)	328 (5670), *374* (6240), 410 (sh, 450), 460 (sh, 2130)
7, **14**	Pt	4-py, H	*360* (3900), 410 (sh, 560)	342 (3760), *474* (5890)

[a] λ_{max} in nanometers, where ϵ is the molar absorptivity. The bands shown in italics are assigned to the ILCT transition.

Table 2. Solvent Dependence of the Luminescence Maxima, Quantum Yields, and Lifetimes of **10**

solvent	$^1\phi$	$^3\phi$	$^1\lambda_{max}$ (nm)	$^3\lambda_{max}$ (nm)	$^{air}\tau$[a]	$^{Ar}\tau$[a]	$k_q(O_2)$ (M^{-1} s^{-1})
DMSO	0.002	0.009	677	732	4.3 (67%) 440 (33%)	4.3 (29%) 3200 (71%)	3.4×10^9
DMF	0.002	0.008	678	738	4.7 (75%) 360 (25%)	4.7 (31%) 2600 (69%)	
acetone	0.002	0.005	694	746	5.2 (82%) 290 (18%)	5.2 (34%) 2300 (66%)	1.4×10^9
$C_2H_4Cl_2$	0.002	0.004	703	763			
dioxane	0.001	0.003	729	769			
toluene	0.001	0.001	735	775			

[a] Lifetimes in nanoseconds, where the values in parentheses are the percent contribution of that species to the overall emission.

Table 3. Solvent Dependence of the Luminescence Maxima, Quantum Yields, and Lifetimes of **14**

solvent	$^1\phi$	$^3\phi$	$^1\lambda_{max}$ (nm)	$^3\lambda_{max}$ (nm)	$^{air}\tau$[a]	$^{Ar}\tau$[a]	$k_q(O_2)$ (M^{-1} s^{-1})
DMSO	0.003	0.03	713	742	3.1 (79%) 460 (21%)	3.1 (24%) 7500 (76%)	3.7×10^9
DMF	0.003	0.03	730	747			
acetone	0.002	0.02	732	755	4.5 (84%) 320 (16%)	4.5 (22%) 5300 (78%)	1.4×10^9
$C_2H_4Cl_2$	0.001	0.009	746	772			
dioxane	0.001	0.007	764	791			
toluene	0.0006	0.003	765	818			

[a] Lifetimes in nanoseconds, where the values in parentheses are the percent contribution of that species to the overall emission.

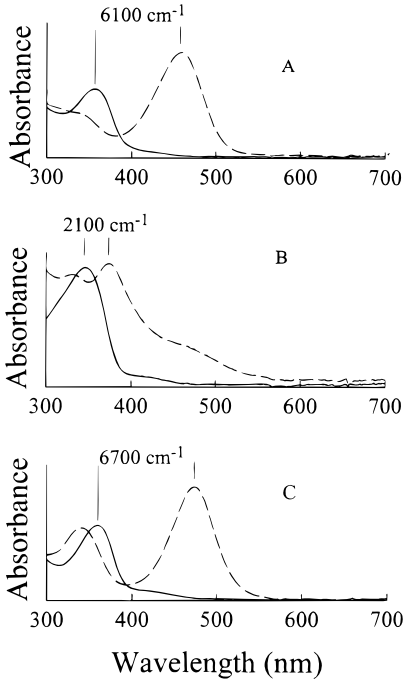

Figure 2. UV−visible absorption spectra: (A) **3** (solid) and **10** (dashed); (B) **6** (solid) and **13** (dashed); (C) **7**(solid) and **14** (dashed). The values shown are the differences in energy of the ILCT transition in the neutral and protonated complexes.

1, Figure 1).[18,19] However, unlike the luminescent quinoxaline-substituted complex,[14b,c] dppePt{S_2C_2(2-quinoxaline)(H)}, where the ILCT band is found at 440 nm, the ILCT band of **1**−**7** is found between 346 and 367 nm and is not the lowest-lying transition in these complexes (Figure 1). The lowest-lying electronic transition in **1**−**7** is metal dependent and is found at 585, 520, and 410 nm for the Ni, Pd, and Pt complexes, respectively. This band is assigned to a d-to-d transition based on the metal dependence, the low molar absorptivity, and the insensitivity of the energy of this band to either the appended heterocycle or solvent polarity.[14b,c]

Although protonation of the heterocycles in **1**−**7** has little effect on the energy of the d-to-d transition, it substantially increases the electron affinity of the heterocycle and, hence, decreases the energy of the 1,2-dithiolate-to-heterocycle π^* charge-transfer (ILCT) transition. However, protonation is not sufficient to lower the energy of the ILCT below that of the d-to-d transition in any of the Ni and Pd complexes or the platinum 3-pyridinium-substituted complex, **13**.[20] In contrast, protonation of **3** and **7** (forming **10** and **14**, respectively) lowers the energy of ILCT below that of the d-to-d transition (Figures 1 and 2).

Only in those complexes where the ILCT transition was lowest in energy (**10** and **14**) did excitation lead to solution luminescence at room temperature (Figure 3). Like (dppe)Pt{S_2C_2(2-quinoxaline)(H)},[14b] deaerated solutions of **10** and **14** exhibit two emission bands that can be assigned to the ^{1}ILCT* and ^{3}ILCT* excited states, based on their relative energies and lifetimes (Tables 2 and 3).

As previously observed for (dppe)Pt{S_2C_2(2-quinoxaline)-(R)},[14b] the addition of air (dioxygen) to solutions of **10** and **14** quenches the ^{3}ILCT* but leaves the ^{1}ILCT* essentially unaffected due to its short lifetime. The quenching of the ^{3}ILCT* by dioxygen decreases its measured lifetime and its

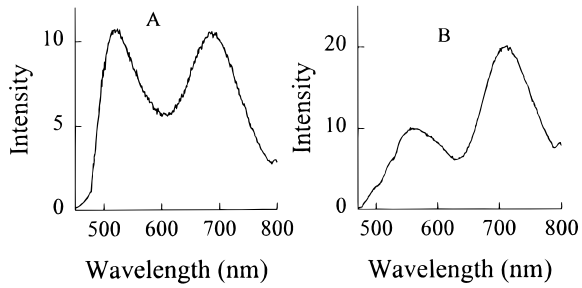

Figure 3. Emission spectra of (A) **10** and (B) **14** in (DMSO) at 298 K under nitrogen prior to instrument correction.

contribution to the total emission (Tables 2 and 3). The second-order rate constants for dioxygen quenching ($k_q(O_2)$) of the ^{3}ILCT* were estimated from the emission percentages (in air and Ar, Tables 2 and 3), the solubilities of dioxygen,[21] and the dioxygen-free lifetime of the ^{3}ILCT*. These values are approximately the same for **10** and **14** and approach the diffusional limit in both acetone ($\sim 1.4 \times 10^9$ M^{-1} s^{-1}) and DMSO ($\sim 3.6 \times 10^9$ M^{-1} s^{-1}).

Quenching of the ^{3}ILCT* by Electron Transfer. Because applications of luminescent metal complexes as switching or sensing devices may use not only luminescence but also excited-state electron transfer as a means of signal transduction, the excited-state electron-transfer reactions of the ^{3}ILCT* of **10** and **14** were examined. Given the long lifetimes of these ^{3}ILCT* and our previous findings for the ^{3}ILCT* of (dppe)Pt{S_2C_2(2-quinoxaline)(H)}, it was anticipated that electron acceptors of the appropriate potential would act as effective quenchers. Electron donors could not be examined because most are sufficiently basic to deprotonate complexes **10** and **14**, thus generating the nonemissive neutral complexes.

The thermodynamic driving force for excited-state electron transfer in DMSO was estimated using

$$\Delta G_e = -E_{oo} + E_{ox} - E_{red} \qquad (2)$$

where E_{oo} for the ^{3}ILCT* was approximated from its emission maximum and E_{ox} and E_{red} are the oxidation potentials of **10** and **14** and the reduction potential of the electron acceptor, respectively. Reduction potentials for *p*-dinitrobenzene (DNB; $E_{red} = -0.48$ V) and tetracyanoquinodimethane (TCNQ, $E_{red} = +0.39$ V) and oxidation potentials for **10** ($E_{ox} = +0.80$ V) and **14** ($E_{ox} = +0.80$ V) were measured in DMSO (where ferrocene/ferrocenium was found at 0.545 V).[22] The thermodynamic driving force for the quenching of the ^{3}ILCT* of **10** and **14** by DNB was predicted to be ~ -0.4 eV, while the driving force for quenching by TCNQ was predicted to be ~ -1.3 eV.[23a] As anticipated from these calculations, both electron acceptors completely quench ($I_o/I \geq 10$) the ^{3}ILCT* emission of **10** and **14** at quencher concentrations of 10^{-3} M. The quenching rate constants, k_q, were nearly identical for **10** and **14** and were found to be 4×10^9 M^{-1} s^{-1} for DNB and 9×10^9 M^{-1} s^{-1} for TCNQ.[23b] Consistent with the calculated thermodynamic driving forces for excited state electron transfer, the k_q values for TCNQ were larger than those for DNB.

(23) (a) In defining triplet energies by their emission maximum, the calculated thermodynamic driving forces for excited-state electron transfer are lower bounds. (b) The k_q values for the quenching of the ^{3}ILCT* of **10** are 4.2(0.8) $\times 10^9$ and 9.4 (1.8) $\times 10^9$ M^{-1} s^{-1}, while those for **4** are 4.1-(0.9) $\times 10^9$ and 8.9(1.7) $\times 10^9$ M^{-1} s^{-1} for DNB and TCNQ, respectively.

Conclusion

The ability to control excited-state reactions through a simple and reversible ground-state reaction (ligand protonation) could prove useful in a variety of applications. In this study, we have demonstrated that members of the (dppe)Pt{S_2C_2(heterocycle)(H)} family of complexes have a long-lived ^{3}ILCT* excited state that is enabled by protonation of the appended heterocycle. Protonation of the heterocycle lowers its reduction potential as well as the energy of the 1,2-enedithiolate-to-heterocycle π^* transition (ILCT). This changes the order of the electronic transitions in the pyridine- and pyridinium-substituted complexes. In the pyridine-substituted complexes, the lower-lying d-to-d transition leads to the rapid nonradiative decay of the excited state, while in the 2- and 4-pyridinium-substituted complexes, the lower-lying intraligand charge-transfer transition allows emission from both the ^{1}ILCT* and ^{3}ILCT*.

While the effects of ligand protonation have been studied in a number of metal chromophores,[13,24−26a-c] we are unaware of any other complex where both luminescence and excited-state electron transfer are reversibly enabled by ligand protonation/deprotonation. In most transition metal chromophores, ligand protonation either quenches the excited state or shifts the emission to lower energy, hence decreasing the thermodynamic driving force for excited-state electron transfer. Recent studies of lanthanide-containing chromophores have demonstrated that luminescence can be cleanly switched on by ligand protonation, but, due to their very positive oxidation potentials, these complexes are not expected to undergo facile excited-state electron transfer.[13]

This study has also expanded our knowledge of the properties of an emerging class of metal chromophores, the platinum 1,2-enedithiolates.[14b,c,26] Our work has concentrated on heterocyclic-substituted 1,2-enedithiolate complexes for which we have developed a new synthetic method.[14c] We have now shown that the excited-state properties of this family of complexes includes protonation-state-dependent luminescence and excited-state electron-transfer reactions, as well as excited-state basicity.[14b]

Acknowledgment. We are indebted to the donors of the Petroleum Research Fund, administered by the American Chemical Society (Grant Nos. 28499-G3 and 32486-AC3), the Exxon Education Foundation, and the Office of the Naval Research (N00014-95-10201) for supporting this work.

Supporting Information Available: Experimental details and spectroscopic characterization for **1**−**7** (4 pages). See any current masthead page for ordering and Internet access instructions.

JA970834Q

(24) Vos, J. G. *Polyhedron* **1992**, *11*, 2285−99 and references found within.

(25) (a) Liu, W.; Thorp, H. H. *J. Am. Chem. Soc.* **1995**, *117*, 9822−5. (b) Liu, W.; Welch, T. W.; Thorp, H. H. *Inorg. Chem.* **1992**, *31* 4044−5. (c) Liu, W.; Thorp, H. H. *Inorg. Chem.* **1994**, *33*, 1026−31.

(26) (a) Cummings, D. S.; Eisenberg, R. *Inorg. Chem.* **1995**, *34*, 2007−14. (b) Cummings, S. D.; Eisenberg, R. *J. Am. Chem. Soc.* **1996**, *118*, 1949−60. (c) Cummings, D. S.; Eisenberg, R. *Inorg. Chem.* **1995**, *34*, 3396−403. (d) Bevilacqua, M. J.; Zuleta, A. J.; Eisenberg, R. *Inorg. Chem.* **1993**, *32*, 3689−93. (e) Bevilacqua, M. J.; Eisenberg, R. *Inorg. Chem.* **1994**, *33*, 2913−23. (f) Zuleta, J. A.; Bevilacqua, J. M.; Eisenberg, R. *Coord. Chem. Rev* **1991**, *111*, 237−48. (g) Zuleta, J. A.; Bevilacqua, J. M.; Proserpio, D. M.; Harvey, P. D.; Eisenberg, R. *Inorg. Chem.* **1992**, *31*, 2396−404. (h) Zuleta, J. A.; Burberry, M. S.; Eisenberg, R. *Coord. Chem. Rev.* **1990**, *97*, 47−64. (i) Zhang, Y.; Ley, K. D.; Schanze, K. S. *Inorg. Chem.* **1996**, *35*, 7102−10. (j) Rosace, G.; Giuffrido, G.; Guglielmo, G.; Campagna, S.; Lanza, S. *Inorg. Chem.* **1996**, *35*, 6816−22.